

Hybrid Post-Tensioned Concrete Shear Walls Behavior Under Seismic Loads

Alshawabkeh Shorouq*, Wu Li**

*Master student, Department of Civil Engineering, Faculty of Engineering, China University of Geosciences, Wuhan, China

** Professor, Department of Civil Engineering, Faculty of Engineering, China University of Geosciences, Wuhan, China

DOI: 10.29322/IJSRP.9.05.2019.p89103

<http://dx.doi.org/10.29322/IJSRP.9.05.2019.p89103>

Abstract- Recent researches and studies have demonstrated that post-tensioned reinforced concrete shear walls have attractive characteristics in resisting lateral loads resulting from seismic forces, such characteristics like self-centering capacity and the ability to experience non-linear horizontal relocations with little harm. The main disadvantage of these wall systems is the small amount of energy dissipation causing an increase in the lateral displacements when experiencing a seismic loading.

This study examines a “hybrid” concrete shear wall system that uses mild steel reinforcement as well as the use of post-tensioned steel for flexural strength and inelastic energy dissipation. A logical parametric examination is carried out in order to compare the expected seismic behavior of the concrete wall subjected to seismic loading in a series of prototype or model hybrid walls of post tensioned steel in a precast concrete shear walls and cast-in-place concrete shear walls. Results have indicated that the use of mild steel in addition to post-tensioned steel in reinforcing the concrete shear wall has enhanced the characteristics of the concrete shear wall regarding resisting seismic forces especially in reducing the lateral displacement (i.e., dislocation) resulting from an earthquake loading.

Combining traditional reinforced concrete structures with post-tensioning technology creates a hybrid concrete wall. The hybrid wall includes mild steel combined with post-tensioned (PT) steel gives many advantages over the traditional reinforced concrete wall such advantages include better energy dissipation and higher self-centering capacity as well as more ductile conduct over lateral dislocations. Subsequently, post-tensioning steel and mild steel both are adding value to the flexural strength of the wall which would result in minimizing the total area of steel required for the needed flexural strength in a traditional reinforced concrete shear wall. The seismic conduct of hybrid unbonded PT concrete walls is examined in this study. ABAQUS software is being utilized with finite element analysis for different hybrid concrete walls. The outcomes of this study demonstrate that the big nonlinear dislocations in post-tensioned shear wall might be decreased by utilizing increasingly mild steel support in the hybrid unbonded PT concrete shear wall system. The PT steel gives a restoring force power that removes the residual deformations after cyclic loading.

Index Terms- Hybrid. Shear wall. Post-tension. Reinforced concrete. Seismic.

I. INTRODUCTION

Concrete shear walls are well-known load resistance structural systems. Concrete shear walls have many advantages in usage as lateral (i.e., horizontal) load resistance structures such as cost-effective, high performance in resisting lateral loads such as seismic loads, thus usage of concrete shear walls is considered the main structures to resist lateral loads as they have proven their superior characteristics in resisting horizontal loads. The main criteria in design that a designer would like to achieve when designing a seismic resistance structures are ductility, strength and stiffness. Concrete shear walls have proven their excellent performance in meeting those criteria (Fintel, 1995).

The ongoing improvement and development of precast concrete techniques because of their building speed and their exceedingly controlled manufacturing has prompted the ongoing precast concrete shear walls process advancement (Chiou, et al., 2006), The precast concrete shear walls design has commonly pursued similar standards utilized for cast-in-place concrete walls, with changes made as suitable for the nature of the precast walls. The hybrid post-tensioned concrete shear walls combine the advantages of both reinforced concrete shear walls and the self-centering ability provided by the post-tensioned steel bars.

The post-tensioned steels bars show a significant resistance improvement against seismic loads, also reduces permanent deformations resulting after earthquake events.

Self-centering capability is the capacity of a structure to return to its original unreformed position after the unloading of a big no-linear movement.

As states earlier post-tensioned wall including only post-tensioning (PT) steel bars do not have enough amount of energy dissipation needed to limit the lateral displacement resulting from seismic loading, hence the need to replace some of the PT steel reinforcement area with mild steel bounded reinforcement, the same strength could be achieved accordance with less non-linear displacement and more dissipation of seismic energy. Area result a total reinforcement steel area (PT reinforcement plus mild steel reinforcement) will be less than the reinforced concrete wall of same flexural strength this may lead to more compact wall dimensions and hence more cost-effective constructions.

This study is focusing on examining the conduct (i.e., behavior) of the hybrid post-tensioned concrete wall experiencing an earthquake loading. The past researches and studies (Kurama 2002, Smith et al 2010 and Chavan et al 2017) were dealing with such wall systems as a precast system consists of separate wall

boards that are fixed together. Meanwhile; this study compares such a precast wall system with another system that is unified unit cast monolithically in place. Never the less; the results of the current study indicate that the hybrid unbonded post tensioned cast in place and the post tensioned precast concrete shear walls are comparable and go along with those results found by previous study for hybrid unbonded precast shear wall systems (Chavan et al,2017 and Shatnawi et al,2018).

Study Limit States

The high-strength unbounded post-tensioned concrete shear walls may experience a significant dislocation without loss of strength (i.e., high ductility) or reduction in self-centering capability. Nevertheless, as expressed prior, post-tensioned walls including just post tensioning (i.e., PT) bars don't give an adequate amount of energy dissipation to resist the dislocations resulting from earthquake loading sufficiently. Thus, substituting a certain portion of the post-tensioning reinforcement steel area with mild steel reinforcement will provide the equivalent flexural strength yet with decreased nonlinear dislocations and improved energy dissipation. Anyway, the total area of steel reinforcement (i.e., PT reinforcement steel area in addition to mild steel reinforcement area) that conveys the flexure strength of the concrete shear wall is not as much as that of the conventional reinforced concrete wall of comparable strength, strengthened concrete wall of; this may prompt increasingly minimized wall measurements (i.e., more compact wall dimensions) which could result in lower costs.

For the unbonded post-tensioning member, the standard suspicion of strain compatibility between the tendon and adjacent concrete couldn't be achieved unlike the bonded system. In the unbonded system, the change in the tendon strain is uniform over the unbonded length of the tendon. At the end of the day, the tendon strain relies upon the change length of the concrete adjacent to the tendon over the unbonded length; the growth in tendon stress, Δf_p , is determined by computing the increment in tendon strain, $\Delta \epsilon_p$ which is determined as the length increasing that happens in tendon after deformation over its original length.

Thus, the tendon stress and the strain are related to the member deformation rather than the section deformation. Thus, when the concrete acquires its ultimate strain at compression face the strain in unbonded tendon, would be lower than if the tendon was bonded to the concrete, and in this manner, the unbonded tendons can achieve the inelastic strain at bigger whole member deformations. Along with the writing referenced before, a few analysts had inspected the conduct of the post-tensioned cast-in-place (PT-CIP) shear walls (Aaleti et al. 2009, Erkmen et al 2009, Henry et al.2012, Hassanli et al,2016, Henry et al.2016). However hardly investigating the execution of hybrid PT-CIP shear walls with mild steel under the impact of the seismic loading.

Structure Limit States and Corresponding Capacities Estimation

For a specified member or area of a structure a force and a deformation limit are determined to stand for the capability of that member or area, this specific limit is being defined as the limit state. The limit states for the hybrid unbonded post-tensioned

concrete walls are presented thru the utilizing the ideal base shear- roof drift relationship appeared in Figure 1.

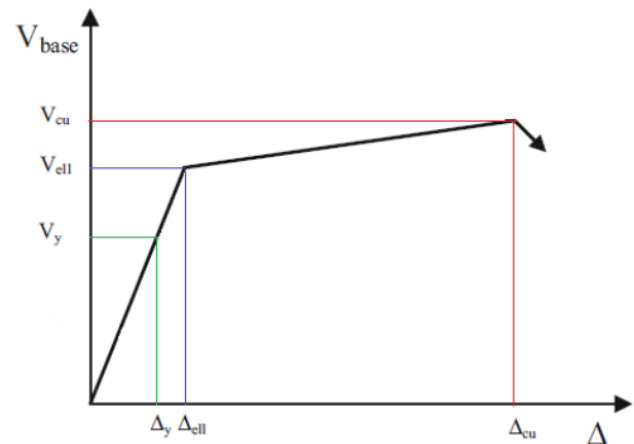


Figure 1: Hybrid unbonded post tensioned wall idealized base shear vs roof dislocation relationship.

Effective Linear Limit of Base Shear-Roof Drift Relationship

(V_{ell}, Δ_{ell})

The horizontal load reaction of the proposed hybrid unbonded PT concrete shear wall is generally straight elastic, until a time when a decrease in the lateral stiffness of shear wall is achieved, such an occurrence is called softening (Kurama,1999). In a hybrid unbonded PT concrete shear wall, softening happens in a smooth and persistent way. Thus, an adequate linear limit for the base shear-roof drift relationship is characterized, and in this investigation, it is allocated when the lowest value of slope *f* the base shear-roof drift starts as appeared in Figure 2.

Softening of a hybrid unbonded PT concrete shear wall may happen because of two reasons: (1) nonlinear conduct of concrete; (2) nonlinear conduct of PT steel in tension. Nevertheless, due to unbonding of the hybrid PT concrete shear wall, nonlinear conduct of PT steel happens after critical horizontal deflection in the wall happens. Along these lines, the viable linear limit of base shear-roof dislocation relationship is controlled by the nonlinear conduct of concrete.

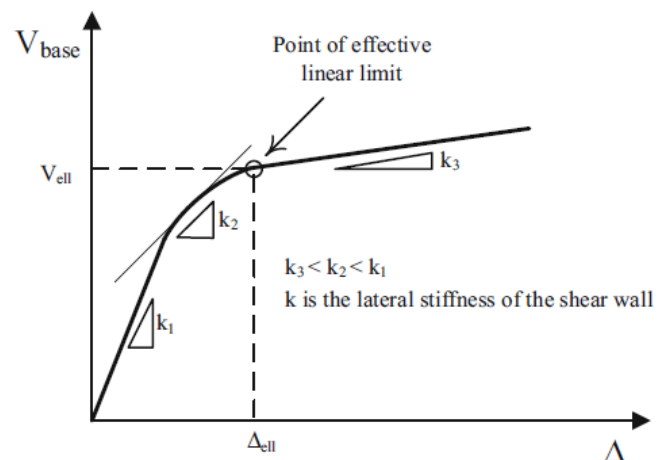


Figure 2: Effective linear limit point on base shear vs roof drift relationship.

The nonlinear distribution of concrete in compression is replaced by the comparable rectangular stress block as permitted by the American Institute of Concrete, ACI 318-14 (American Concrete Institute, 2014). The depth of this square is determined as follows:

$$a = \frac{N_i + A_s f_y - A'_s f'_s}{0.85 f'_c h_w} \quad (1)$$

And so, base moment, M_{base} and base shear, V_{base} are computed as:

$$M_{base} = \frac{1}{2} C (l_w - a) + A_s f_s \left(d - \frac{l_w}{2} \right) - A'_s f'_s \left(\frac{l_w}{2} - d' \right)$$

$$V_{base} = \frac{3}{2H} M_{base} \quad (2)$$

$$C = 0.85 f'_c a h_w = A_s f_y - A'_s f'_s + N_i \quad (3)$$

Where C represents the value of the total compressive stress resultant at wall base, a stands for the depth of the comparable (equivalent) stress block, A_s represents the area of mild steel bars reinforcement in the tension side of the concrete shear wall, A'_s is the mild steel reinforcement in the compression side of the concrete shear wall, f_y is the mild steel yield stress, f'_s is the mild steel stress on the compression side of the concrete shear wall, f'_c is the concrete compressive stress, d represents the distance between the mild steel area's centroid on the tension side and the extreme edge of compression of the wall, d' represents the distance between the mild steel area's centroid on the compression side and the extreme edge of compression of the wall. The base shear and roof drift at softening are given as V_{ell} and Δ_{ell} , respectively.

Yielding of Mild Steel

Mild steel reinforcement is designed so that it would yield in tension in the anticipated hybrid unbonded PT shear wall so that it will limit the maximum nonlinear dislocation, and provide the needed energy dissipation. As the shear wall contains number of mild steel bars distributed at its both sides, this limit state will be defined as the first happening of yielding in these bars. Never the less, the base shear and roof displacement when the mild steel yields are donated as V_y and Δ_y , respectively. At tensile steel level concrete stress is being computed by dividing the yield stress of mild steel by the modular ratio, n calculated as follows:

$$n = \frac{E_s}{E_c} \quad (4)$$

Where E_s is defined as the modulus of elasticity for mild steel and E_c is defined as the modulus of elasticity for concrete.

Yielding of Post-Tensioning Steel

The yielding of post-tensioning steel would happen when the strain value approaches the value of the yield strain of PT steel. Therefore, this limit state occurs only when the PT cast in place shear wall undergoes a significant displacement. The base shear

and roof displacement at yielding of PT steel are donated as V_{py} and Δ_{py} , respectively.

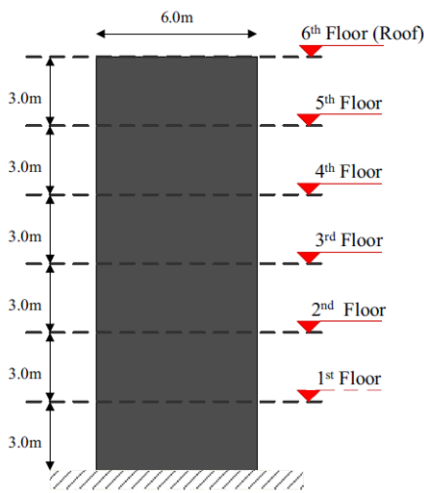
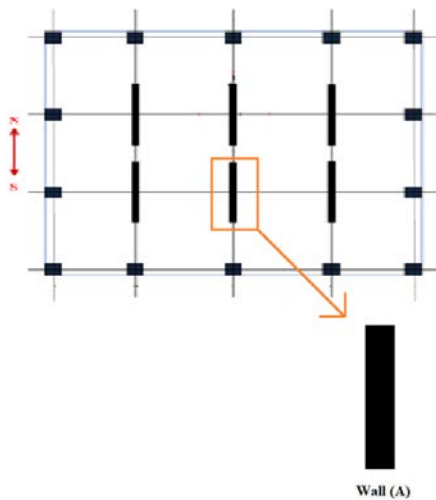
Crushing of Concrete

The failure of shear wall would occur when the concrete at the base of shear wall fails in compression, this happens at an ultimate concrete compressive strain of ϵ_{cu} , this maximum usable concrete strain is specified by ACI318-11 as $\epsilon_{cu} = 0.003$ beyond which the concrete fractures. The base shear and roof dislocation when concrete approaches its ultimate compressive strain are donated as V_{cu} and Δ_{cu} , respectively.

Building Description

The investigation is done on a six-story office building of plan view as appeared in Figure 3; this arrangement looks like the one utilized by Kurama (2005) with modified measurements and number of spans. Tow unbonded mixture PT concrete shear walls give horizontal load resistance; gravity loads are supported by reinforced concrete frames and hybrid PT concrete shear walls. This study focuses on the seismic conduct of one of the inside concrete shear walls (i.e., wall (A) appeared in Figure 3a, that resist the seismic load in the N-S direction. The concrete shear walls in this building are chosen to be having a length, $l_w = 6.0$ m and thickness, $h_w = 0.35$ m. Each floor height is assumed to be equal to 3.0 m which makes the total height of the building, $H = 18$ m as appeared in Figure 3b.

The seismic analysis is being performed with respect to the ASCE/SEI 7-16 (American Society of Civil Engineers, 2016) for a structure of design risk category II and placed over stiff soil (i.e., site class D). The mapped spectral response accelerations were $S_s = 0.50$ g for short period and $S_l = 0.20$ g for 1-s. period; g is defined as the gravitational acceleration. That lead to a seismic design category (C). The allowable story drift was chosen to be $0.020h_{sx}$, in which h_{sx} represents the story height beneath the level x .



(a) (b)
Figure 3: Assumed building configuration in our study, (a) plan view and (b) elevation view of wall A.

Analytical Model

The analytical model suggested in this study for the concrete wall is developed based on previous models developed like the model developed by Kurama et al (1996) and Kurama et al (1999). For instance, Figure 4 demonstrates the analytical model for a six-story wall.

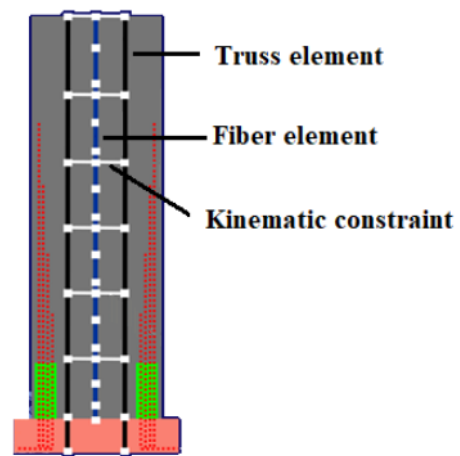


Figure 4: Elevation view of analytical model in our study

The analytical model in this study assumes that the mild steel reinforcement are anchored adequately and fully bonded to the concrete, thus any slip results from bond or anchorage failure is neglected. The assumed stress-strain relationship for the mild steel is shown in Figure 5 this relationship is created depending on experimental results reported by Paulay and Priest (1992).

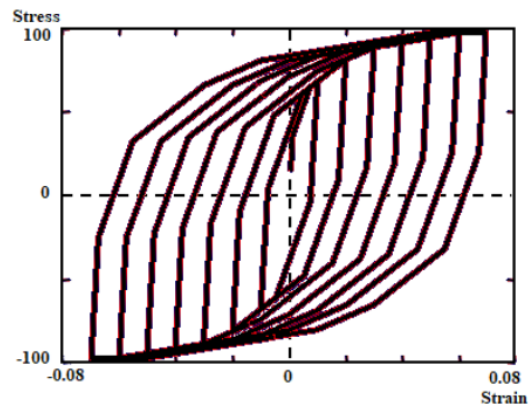


Figure 5: Mild steel of analytical model

Analytical Model Assumptions and Limitations

As depicted in detail by Kurama (1999), the ideal conduct of unbounded post-tensioned precast walls under horizontal loads is controlled primarily, by the opening of gaps along the horizontal joints and, to a less degree, by the axial-flexural deformations of the wall boards.

A great standpoint of utilizing fiber beam-column section components for the wall boards is that an accurate model can be created utilizing just uniaxial stress-strain models for the concrete, post-tensioning steel and mild steel, and the components of the wall. The model referred to as the fiber wall demonstrate, represents the axial- flexural interaction in the wall, the gap opening along the level joints, and the hysteretic conduct of the mild steel, post-tensioning steel, spiral confined concrete, and unconfined concrete fined concrete. Note that buckling and low cycle fatigue crack of the mild steel bars are not demonstrated.

The accompanying presumptions are made for the hybrid PT concrete shear wall model (prototype); the Seismic forces are acting in the long direction of the wall and they are totally resisted by concrete shear walls. Also, the Seismic weights of structures at

each floor level, (i.e., w_x) are equivalent and for the building under investigation, the center of mass and center of rigidity are correspondent, which implies no torsional impacts of earthquakes are integrated. As well as the seismic forces at each floor would be transferred to the walls by floor and roof rigid diaphragm. Hence; the wall experiences a similar lateral distortion at each floor level because of unbending rigid diaphragm statement. Deformations that may happen in the foundation are not counted. Anchorage of the post-tensioning tendons remains completely viable amid the seismic reaction of the walls. Long-term losses in post-tensioning force because of shrinkage and creep not being taken into consideration. The mild steel bars reinforcement is completely attached (bonded) to concrete, which means that any slip or bond failure is not counted.

II. ANALYTICAL MODELING

Selection of Elements

In order to be able to demonstrate the general behavior and some unique characters of the hybrid walls with a general more common and basic analysis technique; a basic Finite Element model was created using the ABAQUS software where a model of monotonic lateral load analysis was implemented. This model has the few assumptions which were made specifically to simplify the analysis and make it more appropriate for the design office, these assumptions include using the yield point to be the measured strength of the unconfined concrete which implies an elastoplastic concrete conduct (i.e., behavior) this assumption makes the Finite Element model unable to capture the concrete cracking, also; using the measured yield strength for the elastoplastic conduct of mild steel, in addition to the previous assumption other assumptions were made such as the rigid or hard contact between base board to foundation joint, and lumped pot tensioned and mild steel areas at the wall centerlines. However; the contact behavior at the base joint and gap opening were modeled. See Figure 6.

ABAQUS software programming (2008) is being utilized to show the proposed model concrete shear wall. An eight-node first-order three-dimensional solid components are utilized to demonstrate the solid concrete wall.

The reinforcing bars are displayed utilizing the three dimensional, two-node truss components embedded inside the concrete components. Post-tensioning tendons are displayed utilizing three-dimensional, two-node beam components demonstrating the strands inside a three-dimensional, two-node pipe component utilizing the external conduits (ducts). These conduits are inserted inside the concrete components. The unbonded tendon slip is being characterized utilizing the three-dimensional single-node internal tube-to-tube component. These components are reasonable for characterizing the collaboration between an external and inner pipe or an external pipe and an internal beam with respect to this case. The default mechanical surface collaboration with the cylinder to-tube contact component is frictionless which agrees to the meaning of unbonded tendons.

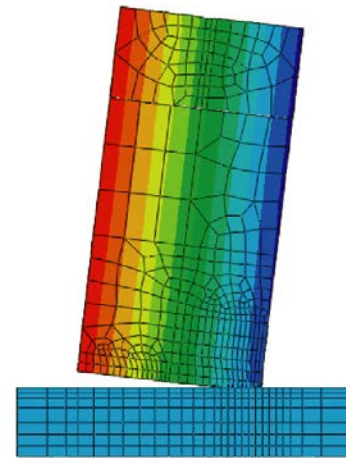


Figure 6: Analytical modeling; finite element (ABAQUS) model.

Boundary Conditions and End Anchorage

The post-tension force's level is dictated by considering dislocation and geometric similarity conditions as opposed to the strain similarity presumptions commonly made in bonded reinforcement. This is on the grounds that strain similarity between the concrete and the unbonded tendons does not exist at the section level. Or maybe, the change in tendon strain is associated to the wall distortion between the two tendon anchorages. For unbonded PT concrete shear walls, the transfer of force from the tendons to the concrete is by methods for the end anchors and the profile of the tendons. The strains in the tendons allocated all through their entire length.

To achieve the above-mentioned conditions, the Beam Multiple-Points Constraint (MPC), which is a built-in function in ABAQUS software programming (2008), is being applied at the end anchorage with the purpose that a rigid component is shaped between the two-node beam elements components (i.e., strands) end nodes and the concrete wall nodes. Plus, fixed boundary conditions are allocated to the nodes of the bottom face of the concrete shear wall. The MPC is likewise used to connect the nodes at the upper and lower floor levels to keep up indistinguishable horizontal dislocation of various floor levels and to guarantee the rigid diaphragms assumption made up earlier. The referenced above conditions guarantee that the deformation and geometric similarity conditions are verified between the PT tendons and the concrete at various strand levels.

Table 1: properties of the material that used in the analytic model

Propert y	Concrete	Mild steel	PT steel
Mass density (kg/m ³)	2400	7860	7860
Poison ratio, ν	0.200	0.303	0.303
Modulus of elasticit	29,725	200	190,000

y, E (MPa)			
Strength	$f'_c = 40$	$f_y = 414$	$f_{py} = 1670$
Strain	$\epsilon_{cu} = 0.00300$	$\epsilon_y = 0.00207$	$\epsilon_{py} = 0.0879$

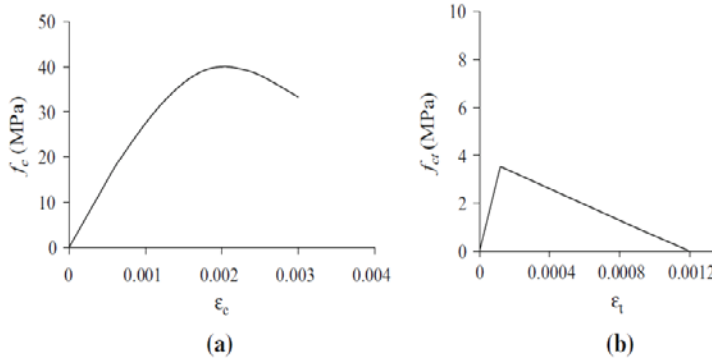


Figure 7: Stress-strain model of concrete under (a) Compression loads and (b) Tensioned loads.

Materials Properties

Three materials are characterized for the concrete shear wall model demonstrate: concrete, mild steel, and high-strength PT steel. The materials characteristics and properties are elaborated beneath and showed in Table 1.

Concrete

A concrete cylinder compressive strength of 40MPa is estimated, the uniaxial stress– strain models for this material under both compressive and tensile forces are shown in Figure 7.

The nonlinear material conduct of concrete in ABAQUS is portrayed utilizing the material model "concrete damaged plasticity". This model is characterized by utilizing concrete damaged plasticity, concrete compression hardening, and concrete tension stiffening choices. The conduct of stress-strain of the concrete under uniaxial compressive loading could be divided into three zones. The principal zone demonstrated by the linear-elastic branch, which can be figured as a direct linear-elastic function of the modulus of elasticity:

$$f_c = E_c \epsilon_c \tag{5}$$

Where E_c for $f'_c = 40MPa$ equivalent to $E_c = 4700\sqrt{40} = 29,725MPa$ f_c is the compressive stress of concrete.

This linear branch closes at about 0.45 f'_c according to American Concrete Institute (2014), and it is characterized utilizing "elastic" alternative accessible inside ABAQUS (2008) The second zone is determined by the ascending branch up to the estimation of f'_c that is 40MPa, come to a strain value equal to $\epsilon_o = 0.002$. The third zone is shown by the post yielding branch which is finished by greatest usable value of concrete solid strain $\epsilon_{cu} = 0.003$ indicated by American Concrete Institute (2014), The nonlinear compressive conduct of concrete (i.e., second and third

zones) is characterized utilizing "concrete compression hardening" choice.

As well as, under tensile loading in order to characterize the uniaxial stress– strain model of concrete; the concrete tension stiffening choice is utilized, this choice is important to characterize the relation and interaction between the concrete and the reinforcing bars when cracking happens (2008). The stress– strain curve defined to by this model is displayed in Figure 7b. This curve is divided into two lines associated at the estimation value of elasticity of concrete, f_{ct} that is estimated American Concrete Institute (2014), as pursues:

$$f_{ct} = 0.56\sqrt{f'_c} \tag{6}$$

Which equals to 3.5 MPa for $f'_c = 40MPa$

The stress–strain curve is linear elastic below this value, and the tensile strains can be computed giving the following equation:

$$\epsilon_t = \frac{f_t}{E_c} \tag{7}$$

Where f_t is the tensile stress of concrete.

From the equation above, it could be acquired that the most extreme value for tensile strain for the concrete model is equivalent to 0.012%, and this esteem is representing the failure strain of concrete. After the failure point, a stiffening curve is ought to be characterized to represent the strain softening conduct for cracked concrete and to incorporate the impact of the reinforcement interaction with concrete. For relatively heavy reinforced concrete, tension stiffening is proposed as the pressure is decreased to zero at a total strain of around ten times the strain failure (2004). This maximum upper limit is expected for the present model as appeared in Figure 7 so as to consider the presence of high-strength PT reinforcement in addition to the conventional mild steel reinforcement.

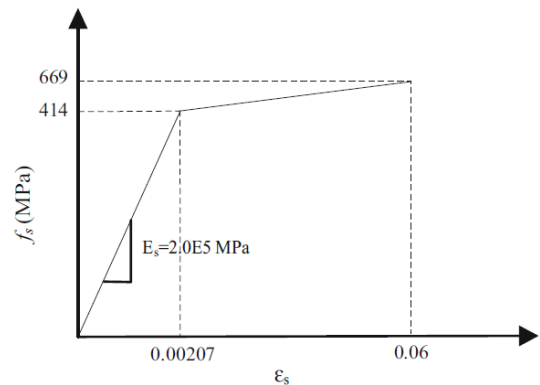


Figure 8: Mild steel stress-strain curve.

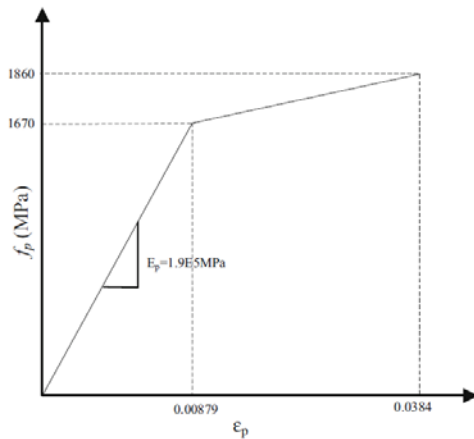


Figure 9: Post tensioned steel stress-strain curve.

Mild Steel

A bilinear model is appeared in Figure 8 , and it is assumed for demonstrating the stress– strain conduct of mild steel. Properties of mild steel are equivalent to the values that are embraced by Kurama (2002), in which the ultimate strength and the yield strength are assumed to be equivalent to the values with $f_y = 414$ MPa and $f_u = 669$ MPa, respectively. The elastic choice is utilized to characterize the linear section up to the yielding point. Never the less, post-yielding zone is demonstrated utilizing the "plastic" choice, which is utilized to recognize the plastic part of the elastic– plastic material. By incorporating the kinematic hardening parameter to the plastic choice, the bilinear model is shown in Figure 9.

Post-Tensioned Steel

Tendons Grade 1860 seven-wire strands are utilized in this investigation; the stress– strain relationship is appeared in Figure 9, and it is demonstrated as a bilinear model in the similar way as the mild steel reinforcement utilizing the plastic alternative with kinematic hardening parameter to show the post-yielding conduct.

Modeling of Loads

The loads which are incorporated into the wall model are three types of loads, according to the American Society of Civil Engineers (i.e., ASCE): Minimum Design Loads for Buildings and Other Structures, ASCE/SEI 7-16 (2016) and ACI 318-14 (2014):

1. Post-tensioning force
2. Gravity loads.
3. Lateral (horizontal) loads.

In the examination of hybrid PT concrete shear wall model, the three loads are imposed so that to isolate progressive steps starting with the post-tensioning force, then the gravity loads, lastly the equivalent static horizontal loads.

Post-Tensioning Force

The post-tensioning force is displayed in the model utilizing the initial condition choice gave in (ABAQUS, 2008). Jacking stress esteem is chosen considering the prerequisites of ACI 318-14 (American Concrete Institute, 2014); that the tensile stress in prestressing shall not be greater than $0.94 f_{py}$, as well as not more than $0.80 f_{pu}$, where f_{py} and f_{pu} are yield stress and ultimate stress for the PT steel, respectively. An effective stress esteem, f_{pe} of equivalent to $0.49 f_{pu}$ is anticipated for this examination; this

esteem is after allowance for all prompt (immediate) prestress loss. By imposing the initial condition type stress, the post-tensioning stress could be transferred from the end anchorage (MPCs) to the concrete, causing the pre-compressive stress in concrete ($f_{pe} = P_e/A_c$), where P_e is the post-tensioning steel area multiplied by f_{pe} and A_c is the concrete wall cross-sectional area.

Gravity Loads

Gravity loads comprise of the superimposed dead and live loads conveyed by the wall dependent on the suitable tributary from Figure 9.

Live load is load as indicated by the Building Code Requirements for Structural Concrete as minimum design load for an office building (American Concrete Institute, 2014). This esteem is observed to be 2.5 kN/m^2 while the superimposed dead load is taken equivalents to 3 kN/m^2 . These gravity loads are characterized as a surface load applied at every story level.

Horizontal (Lateral) Load

The seismic load is applied utilizing equivalent horizontal force technique. The structure base shear portion resisted by wall (A) [see Figure 3] is determined with no consideration of any torsion that might be brought about by the eccentricity, e . The static horizontal load is shown as a concentrated nodal force at the highest point (i.e., top) of the cantilever shear wall. After the horizontal force is applied, the base shear is determined and after that distributed at every story level as indicated by Building Code Requirements for Structural Concrete (American Concrete Institute (2014)) as illustrated in Figure 10.

In a static technique in ABAQUS/Standard, the default load function is linearly increasing over an examination step; this implies that load is linearly increased with time at every increment until achieving the predefined esteem toward the finish of the step.

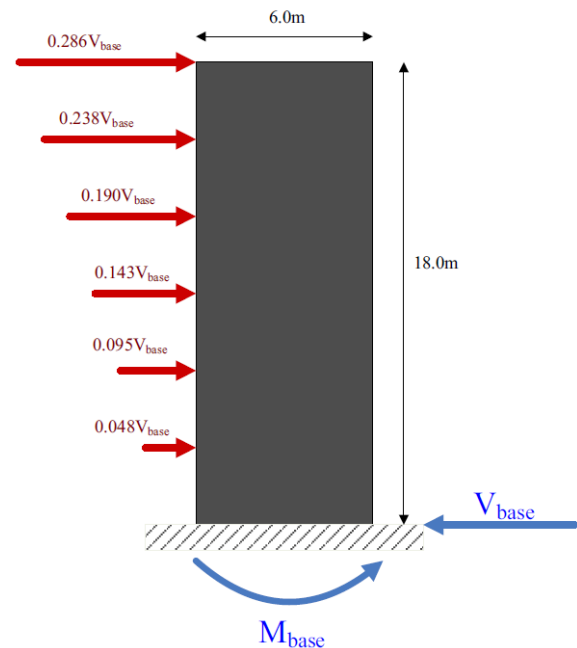


Figure 10: Wall base shear vertical distribution.

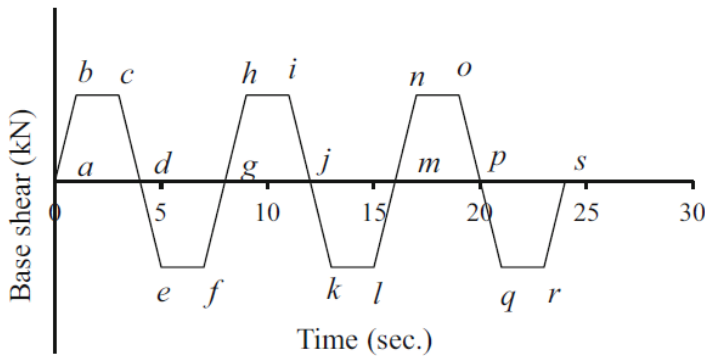


Figure 11: Cyclic horizontal load.

To examine the cyclic conduct of hybrid unbonded PT concrete wall, a second situation where a non-default load function appeared in Figure 11 according to Kurama (2002) is characterized. In this model, each load cycle comprises of loading branch at which horizontal load linearly increased with time to greatest (yielding) value. A constant loading branch is at which the horizontal load holds constant, unloading branch at which the load is linearly decreased to zero parallel to that of loading line, and lastly the loading is reversed.

Six model (prototype) concrete shear walls are examined in this study under proportionate static and static cyclic horizontal load. The flexural strengths of these walls are equivalent. Wall HP1 is a hybrid unbonded PT precast shear wall with A_p / A_s equal to 50%, HP2 is a hybrid unbonded PT precast shear wall with A_p / A_s equal to 75% wall, HC1 is hybrid unbonded PT cast-in-place shear wall with A_p / A_s equal to 50% wall, HC2 is hybrid unbonded PT cast-in-place shear wall with A_p / A_s equal to 75% wall, RC is standard reinforced concrete shear wall and PT is a typical unbonded post tensioned concrete shear wall. A proportion A_p / A_s is embraced for the examination the conduct of hybrid unbonded PT shear walls, where A_p is the post-tensioning steel area and A_s is the mild steel area.

III. RESULTS

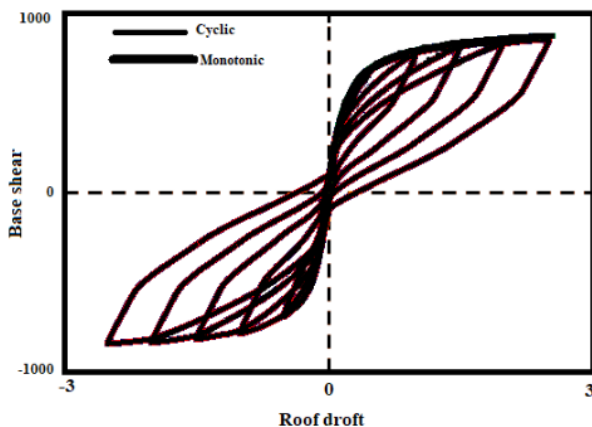


Figure 12: Model walls behavior under horizontal loads.

Figure 12 demonstrates the normal base shear versus roof drift ($V - \Delta$) conduct of the model (prototype) walls under joined gravity loads and reverse cyclic horizontal loads (Kurama, 2002). The gravity loads following up on each wall are thought to be equivalent to $1.00D + 0.25L$, where D and L are the unfactored design dead load and the unfactored unreduced structure live load, individually. This mix of dead and live loads is expected to denote to the measure of gravity load that might follow up on the walls during a seismic loading.

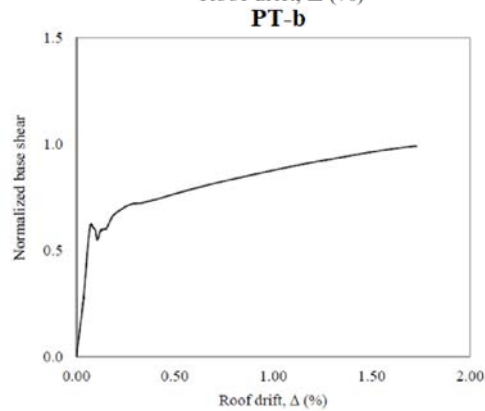
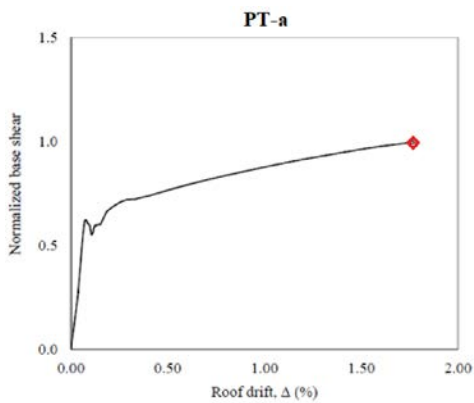
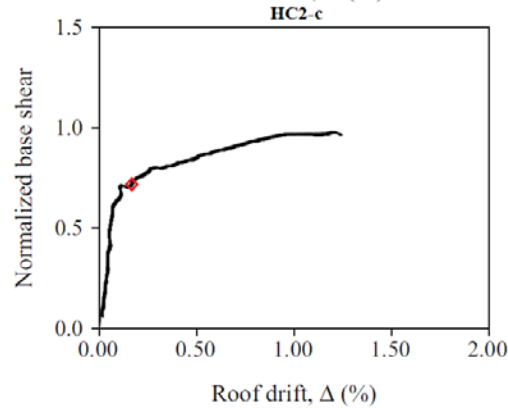
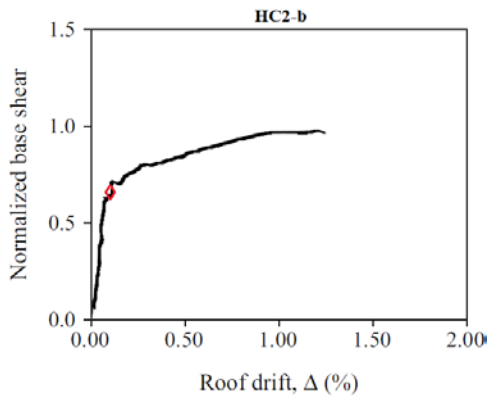
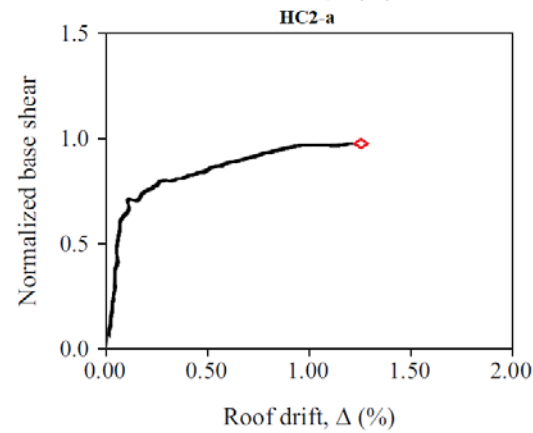
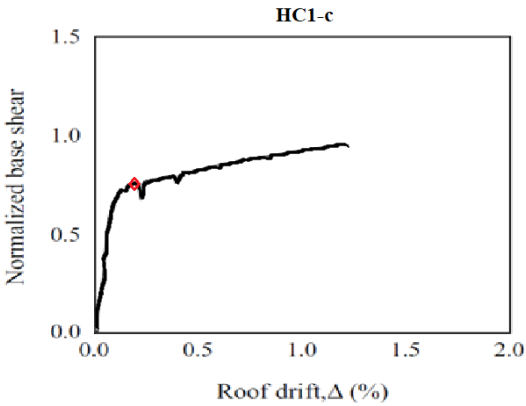
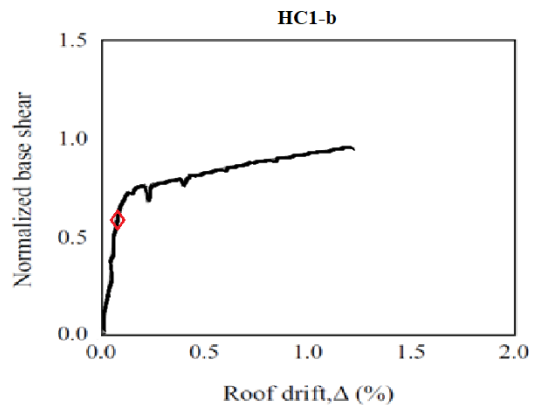
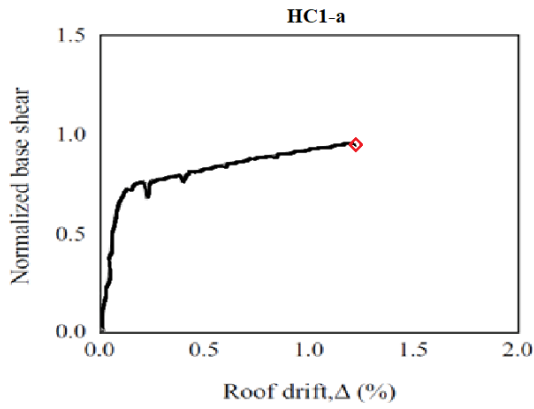
The thick line in Figure 12 demonstrates the base shear versus roof drift conduct of the model wall under consolidated gravity loads and monotonic horizontal loads as acquired from static push-over examinations explained by Kurama (kurama,2002).

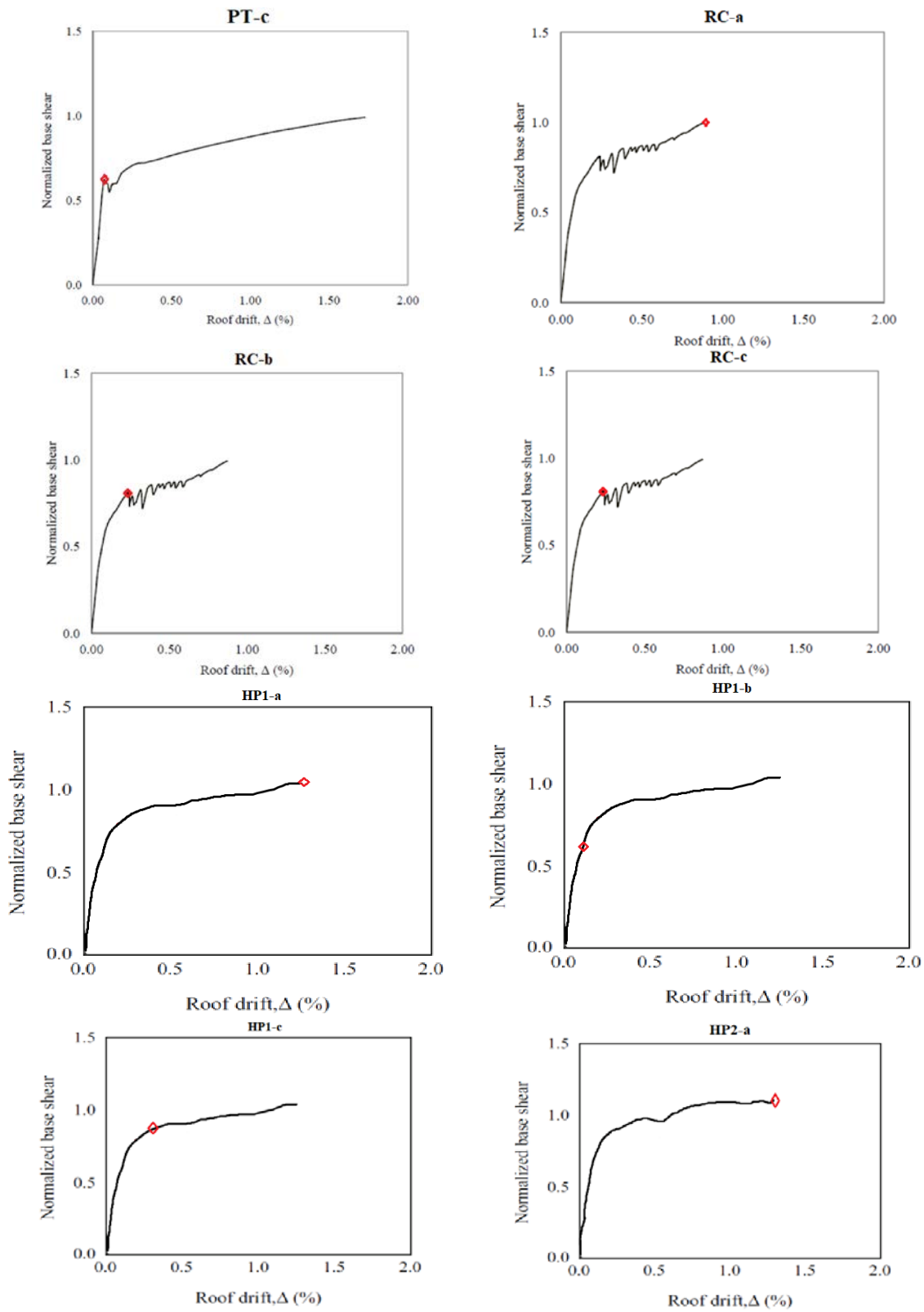
The base shear, V, is equivalent to the aggregate of the horizontal forces employed at the floor and rooftop levels, and the roof drift Δ , is equivalent to the horizontal dislocation at the rooftop level over the wall height. The dispersion of the horizontal forces divided by the height of the walls is thought to be equivalent to the dissemination of inertial forces comparing to the principal (i.e., first) mode of vibration from a linear elastic modular examination of each structure. It's observed that inertial force dissemination is greatly various from the expected basic mode dispersion divided by the height of the walls during a massive seismic loading, but this isn't explored in this study.

Figure 13 demonstrates the base shear versus roof drift connections of the model hybrid HP1, HP2 HC1 and HC2 walls, As known, the increase of the mild steel reinforcement quantity will cause an increase of the amount energy dissipation of the walls.

As expressed before, limit states are considered for the hybrid unbonded PT concrete shear wall; each limit state is demonstrated on the standardized base shear-roof drift plot below:

(RC: Conventional reinforced concrete shear wall, PT: Traditional post-tensioned concrete shear wall, HC1: Hybrid unbonded post-tensioned cast-in-place concrete shear wall with $A_p/A_s=50\%$, HC2: Hybrid unbonded post-tensioned cast-in-place concrete shear wall with $A_p/A_s=75\%$, HP1: Hybrid unbonded post-tensioned precast concrete shear wall with $A_p/A_s=50\%$, HP2: Hybrid unbonded post-tensioned precast concrete shear wall with $A_p/A_s=75\%$).





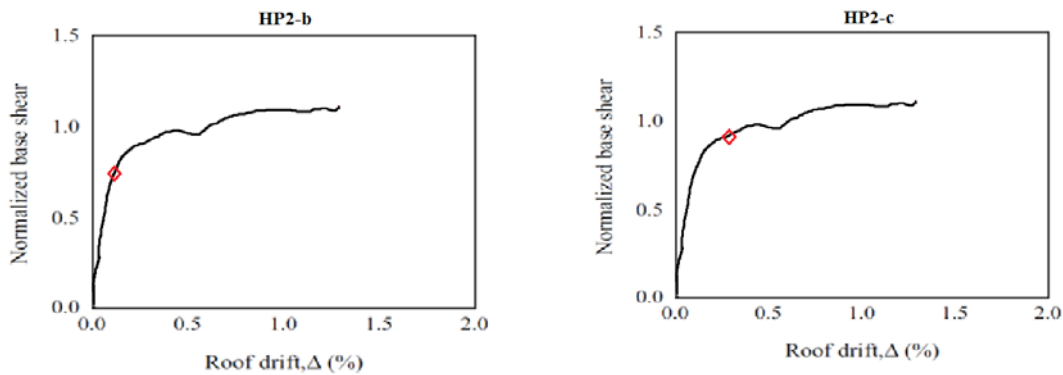


Figure 13: Model walls base shear vs roof drift under static horizontal load. a: crushing of concrete, b: yield of mild steel and c: effective linear limit.

Model walls base shear vs roof drift under static horizontal load results are summarized in the table 2 below.

Table 2: Summary Results of the walls base shear vs roof drift under static horizontal load.

Wall Type	Wall Name	A_p/A_s percentage	V_{cu} (a)	Δ_{cu} % (a)	V_y (b)	Δ_y % (b)	V_{ell} (c)	Δ_{ell} % (c)
Reinforced Concrete	RC	–	1	0.94	0.76	0.21	0.74	0.22
Post tensioned	PT	–	0.97	1.72	–	–	0.59	0.06
Hybrid cast in place	HC1	50%	0.98	1.28	0.69	0.14	0.81	0.22
	HC2	75%	0.96	1.34	0.61	0.11	0.78	0.18
Hybrid precast	HP1	50%	0.97	1.39	0.76	0.13	0.82	0.29
	HP2	75%	0.99	1.43	0.69	0.12	0.79	0.27

The Behavior of Hybrid Unbonded PT Walls Subjected to Equivalent Static Loading

Figure 13 demonstrates the standardized base shear, V_{base} versus the horizontal roof drift, $\Delta\%$ relationships got from horizontal load investigation for the six model walls (i.e., walls, HP1, HP2, HC1, HC2, PT and RC). Rooftop drift is characterized as the horizontal dislocation over the shear wall height. As referenced beforehand, the model walls have an emulative ultimate flexural strength (i.e., have similar V_{cu}). The parametric reaction amounts for these walls are given in Fig. 18. Base shear esteems are standardized by the greatest value of base shear of the reinforced concrete wall RC (i.e., V_{cu}).

The results in Figure 13, demonstrates the extensive decrease in this amount because of utilizing the high-strength PT steel reinforcement. In this way, an ideal flexural strength can be

accomplished however with lower area of reinforcement when a portion of the conventional mild steel is supplanted by a high-strength PT steel. Looking at Figure 13 demonstrate that despite the fact that V_{cu} is equivalent for the model walls, the variety of A_p / A_s proportion prompted diverse values for the rest of parametric reaction amounts. Each of the reaction amount is being discussed below.

Effective Linear Limit

At the base shear and roof drift achieve the estimations of V_{ell} and Δ_{ell} , respectively, a drop in the wall stiffness happens. As A_p / A_s proportion changes, the terms $N_i, A_s f_s, A'_s f'_s$ in Equations. (1) through (3) will change. Looking Figure 13,

outlines that the variety of these terms prompted a decrease in V_{ell} and Δ_{ell} amounts as A_p/A_s proportion increases.

Behavior of Hybrid Unbonded PT Walls Subjected to Static Cyclic Loading

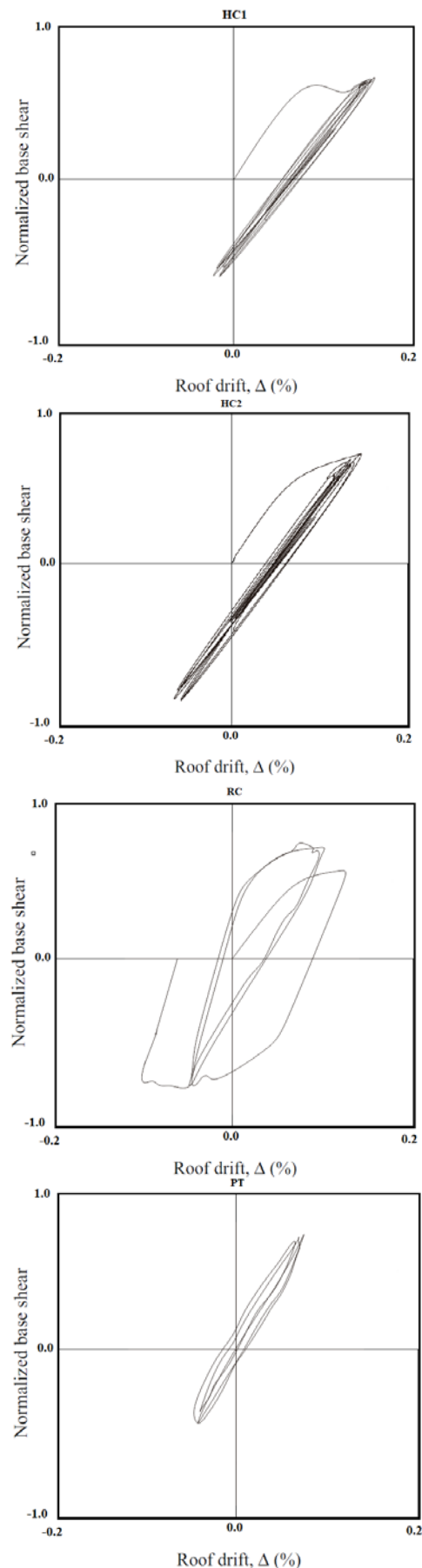
For every wall of the six model walls (i.e., HC1, HC2, HP1, HP2, PT and RC) are exposed to the reversed cyclic loading showed in Figure 11. Each of the three load cycles comprises of loading the wall with linearly increased horizontal load up to a most extreme esteem equivalents to V_y given for each wall in Figure 13, hold constant, and after that the loading is reversed to $-V_y$ and at that point unloading.

For the post tensioned wall PT, the limit state of mild steel yielding isn't given since no mild steel reinforcement exists for this wall. Additionally, it is noted from Figure 13 that yielding of post-tensioning steel happens at a similar base shear at which the concrete crushes (i.e., $V_{cu} = V_{py}$). The advantage of this is that the post-tensioning steel stays elastic in which gives a restoring force to the PT shear wall that enhances its cyclic conduct as will be outlined later. Hence, a yielding base shear, V_y equivalents to $0.60V_{cu}$ is expected for the use of cyclic loading for this shear wall.

Base Shear-Roof Drift Relationship

The standardized base shear versus roof drift relationship for each wall of the six model walls for, when exposed to reversed cyclic loading, are appeared in Figure 14.

The dissipated energy for each wall considered by the area of hysteresis circle (i.e., the region under $V_{base} - \Delta$ curve). It is demonstrated that the biggest hysteresis loop is acquired in Figure 14 (RC) using reinforced concrete wall RC, reinforced concrete wall dissipates energy through yielding of mild steel reinforcement. The dissipated energy is decreased gradually with the increase in A_p/A_s for the concrete shear walls as appeared in Figure 14 as the area under $V_{base} - \Delta\%$ curve ends up smaller until achieving the instance of linear and almost elastic conduct. It is noticed the that largest dissipated energy for the hybrid walls happens at the first loop and after that declines for the second and third loops as the mild steel yields at the first loop and structure lose its strength and subsequently the amount of energy dissipated is minimized in the accompanying loops.



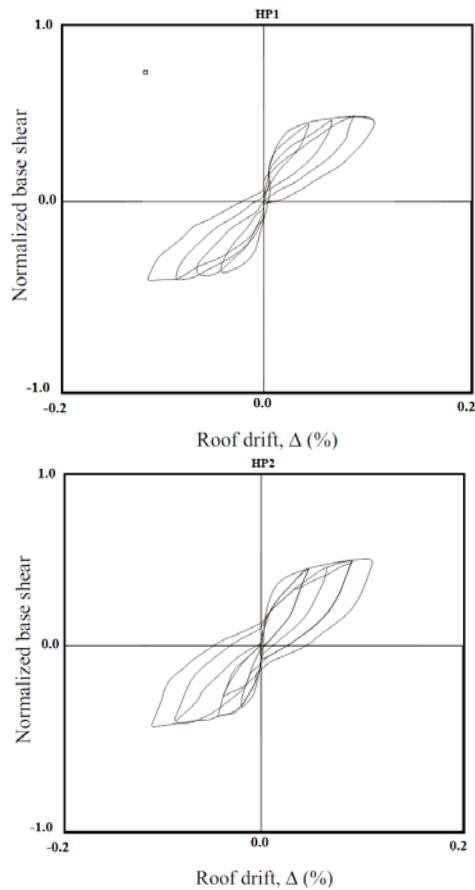


Figure 14: Model walls base shear vs roof drift under cyclic load.

IV. RESIDUAL DRIFT

Figure 14 demonstrates that roof drifts amid the cyclic stacking; it is noticed that removal tops achieved each cycle are the best for wall RC and turns out to be less for HP1, HP2 and HC1, HC2 as A_p/A_s proportion increments. However, as A_p/A_s proportion diminishes, a plastic twisting happens when first greatest sidelong power is come to. That is the point at which the parallel burden connected to the divider achieves its first most extreme esteem ($+V_y$) turns around to another greatest esteem ($-V_y$) some plastic happens in the principal heading, and accordingly, the divider does not achieve a similar horizontal relocation inverse way. The remaining disfigurements toward the finish of three cycles versus A_p/A_s proportion, for every one of the six shear walls, are appeared in Fig. 20. It is noticed that the roof drift is greatest for wall RC and reduced gradually for walls HP1, HP2, HC1 and HC2 as the proportion A_p/A_s increments. It's expected that as A_p/A_s proportion increases until maximum value the bounded occurs which is identified with the extensive restoring force given by the flexible PT tendons that make the shear wall swing back to its unique position.

V. CONCLUSION

The outcomes of past examinations (Kurama 2002) demonstrate that impressive decreases in the horizontal dislocations of post-tensioned precast walls under seismic loading can be accomplished by utilizing bonding mild steel support crossing the horizontal joints of the walls. Similarly, in this study, hybrid precast concrete walls stand for an important feasible essential lateral load resisting structure to be used in seismic areas.

In this study it is shown that the quantity of mild steel reinforcement that is needed in a wall will be depending on the needed decreases in the horizontal dislocations.

Comparing to cast-in-place reinforced walls, the quantity of mild steel that would be required in a hybrid precast wall is less due to the fact that a part of the flexural strength of the wall to resist horizontal loads is given by the post-tensioning steel.

Past researches (Kurama 2002) show that, mild steel reinforcement isn't required for walls in areas with moderate seismicity. Further investigation is expected to be done for walls in areas with high seismicity, an extended research should be applied in order to obtain a seismic design methodology for the mild steel reinforcement to accomplish an objective decrease in the horizontal dislocations, like the plan approaches produced for walls with supplemental friction dampers and viscous fluid dampers as designated by Kurama (2000, 2001).

The most vital horizontal joint for the utilization of bonded mild steel support reinforcement is the base-board to-foundation joint. The reinforcement utilized in a wall has to be adequately anchored to the base (foundation) and also has to be stretched out (extended) to an adequate height over the base of the wall to take into consideration the progression of the yield strength of the steel in tension and compression at the base-board to-foundation joint. This study has explored the predicted seismic conduct of hybrid precast and cast-in-place concrete model walls with various measures of unbonded post-tensioning steel and mild reinforcement steel support.

The Analysis outcomes of reversed cyclic loading show that the inelastic energy dissipation of the hybrid post tensioned cast in place and precast walls is improving by utilizing an increased mild steel area as this mild steel area would through yielding provides better energy dissipation, as noted the self-centering ability would be increased as the proportion A_p/A_s increases and thus the permeant deformation that happens after loading would be reduced.

By utilizing unbonded post-tensioned reinforcement in the hybrid concrete wall the total reinforcement area would be reduced which allows the wall to experience a larger nonlinear horizontal drift compared to a standard reinforced concrete shear wall having the same comparable flexural strength, hence an improvement in the wall ductility would occur. On the other hand, the advantage of hybrid shear wall over a traditional PT wall would be the fact that in a hybrid wall a part of the post-tensioned bars are replaced by mild steel bars this would limit the maximum values for drifts to a desired value with the same base shear capacity.

The outcomes of the analysis of the hybrid wall having different A_p/A_s ratios but with the same flexural strength subjected to equivalent static loads show that when the ratio A_p/A_s increments, the base shear values (V_y and V_{ell}) would be lower, and Δ_{cu} will increase, however Δ_{ell} and Δ_y will decrease.

Note that the different distribution of the strands has no major impact on the the hybrid shear wall behavior. The outcomes of the examination show that the value of base shear (V_{cu} and V_{ell}) could be increased by increasing the amount of post-tensioning steel over that of mild steel, and by increasing the effective prestressing force, also by increasing concrete strength, as well as increasing the thickness of shear wall. On the other hand, the value of Δ_{cu} could be decreased by increasing the effective prestressing force, and increasing the content of mild steel reinforcement, also reducing the thickness of shear wall, as well as reducing concrete strength.

REFERENCES

- [1] Aaleti S, Sritharan S. A simplified analysis method for characterizing unbonded post-tensioned precast wall systems. *Eng. Struct.*, 2009, 31(12): 2966-2975.
- [2] ABAQUS Analysis User Manual, Version 6.8. Dassault Systems Simulia Corp. Providence, Rhode Island, USA, 2008.
- [3] American Concrete Institute: ACI Committee 318, Building Code Requirements for Structural Concrete and Commentary, ACI 318-14. Farmington Hills, MI 2014.
- [4] American Society of Civil Engineers: Minimum Design Loads for Buildings and Other Structures, ASCE/SEI 7-16, 2016.
- [5] Chavan R, Kannan M. Analysis and design of vertical posttensioned precast shear wall. *IJRITCC*, 2017, 5(4): 50-54.
- [6] Cheok G, Stone W, and Nakaki S. "Simplified Design Procedure for Hybrid Precast Concrete Connections," NISTIR 5765, National Institute of Standards and Technology, Gaithersburg, MD, 1996, 81 pp.
- [7] Chiou Y J, Liou Y W, Huang CC, Hsiao F P. 4th International Conference on Earthquake Engineering, Seismic Behavior of Precast Reinforced Concrete Walls, 2006, No.121.
- [8] Erkmen B, Schultz AE. Self-centering behavior of unbonded, post-tensioned precast concrete shear walls. *J. Earthq. Eng.*, 2009, 13(7): 1047-1064.
- [9] Fintel, Mark. Performance of Buildings with Shear Walls in Earthquakes of the Last Thirty Years, *PCI Journal*, 1995, 40(3): 62-71.
- [10] Hassanli R, ElGawady M A, Mills J E. Force-displacement behavior of unbonded post-tensioned concrete walls. *Eng. Struct.*, 2016, 106: 495-505.
- [11] Henry R S, Brooke N J, Sritharan S, Ingham JM. Defining concrete compressive strain in unbonded post-tensioned walls. *ACI Struct. J.*, 2012, 109(1): 101-111.
- [12] Henry R S, Sritharan S, Ingham J M. Finite element analysis of the PreWEC self-centering concrete wall system. *Eng. Struct.*, 2016, 115: 28-41.
- [13] Kurama Y, Pessiki S, Sause R, Lu L W, El-Sheikh M. "Analytical Modeling and Lateral Load Behavior of Unbonded Post-Tensioned Precast Concrete Walls," Research Report No. EQ-96-02, Department of Civil and Environmental Engineering, Lehigh University, Bethlehem, PA, 1996, 191 pp.
- [15] Kurama Y. "Simplified Seismic Design Approach for Friction-Damped Unbonded Post-Tensioned Precast Concrete Walls," *ACI Structural Journal*, V. 98, No. 5, September-October 2001, pp. 705-716.
- [16] Kurama Y, Sause R, Pessiki S, Lu L W. "Lateral Load Behavior and Seismic Design of Unbonded Post-Tensioned Precast Concrete Walls," *ACI Structural Journal*, V.96, No. 4, July-August 1999, pp. 622-632.
- [17] Kurama Y, Pessiki S, Sause R, Lu L W. "Seismic Behavior and Design of Unbonded Post-Tensioned Precast Concrete Walls," *PCI JOURNAL*, V. 44, No.3, May-June 1999, PP. 72-89.
- [18] Kurama Y. "Seismic Design of Unbonded Post-Tensioned Precast Walls with Supplemental Viscous Damping," *ACI Structural Journal*, V. 97, No. 4, July-August 2000, pp. 648- 658.
- [19] Kurama Y. Hybrid post-tensioned precast concrete walls for use in seismic regions. *PCI J*, 2002, 47(5): 36-59.
- [20] Kurama, Y. Seismic design of partially post tensioned precast concrete walls. *PCI J*, 2005, 50(4): 100-125.
- [21] Paulay P, Priestley M. *Seismic Design of Reinforced Concrete and Masonry Buildings*, John Wiley & Sons, Inc., New York, NY, 1992.
- [22] Shatnawi Anis, et al. "Seismic Behavior of Hybrid Post-Tensioned Cast in Place Concrete Shear Walls." *Arabian Journal for Science and Engineering*, Springer Berlin Heidelberg, 2018, doi:10.1007/s13369-018-3281-4.
- [24] Smith B, McGinnis M, Kurama Y. 3rd fib International Congress, Full-Field Lateral Response Investigation of Hybrid Precast Concrete Shear Walls, 2010.

AUTHORS

First Author – Alshawabkeh Shorouq, Master student, Department of Civil Engineering, Faculty of Engineering, China University of Geosciences, Wuhan, China, shorou2.m@hotmail.com, phone number: 0086-18674044095
Second Author – Wu Li, Professor, Department of Civil Engineering, Faculty of Engineering, China University of Geosciences, Wuhan, China, lwu@cug.edu.cn